

**2002**

**NASA FACULTY FELLOWSHIP PROGRAM**

**MARSHALL SPACE FLIGHT CENTER  
THE UNIVERSITY OF ALABAMA**

**ENHANCEMENT AND EXTENSION OF POROSITY MODEL IN THE FDNS-500  
CODE TO PROVIDE ENHANCED SIMULATION OF ROCKET ENGINE  
COMPONENTS**

Prepared By:	Gary Cheng
Academic Rank:	Assistant Professor
Institution and Department:	University of Alabama at Birmingham Department of Mechanical Engineering
NASA/MSFC Directorate:	Transportation
MSFC Colleagues:	Kevin Tucker, Jeff West, Roberto Garcia

## **Introduction**

In the past, the design of rocket engines has primarily relied on the cold flow/hot fire test, and the empirical correlations developed based on the database from previous designs. However, it is very costly to fabricate and test various hardware designs during the design cycle, whereas the empirical model becomes unreliable in designing the advanced rocket engine where its operating conditions exceed the range of the database. The main goal of the 2<sup>nd</sup> Generation Reusable Launching Vehicle (GEN-II RLV) is to reduce the cost per payload and to extend the life of the hardware, which poses a great challenge to the rocket engine design. Hence, understanding the flow characteristics in each engine components is thus critical to the engine design. In the last few decades, the methodology of computational fluid dynamics (CFD) has been advanced to be a mature tool of analyzing various engine components. Therefore, it is important for the CFD design tool to be able to properly simulate the hot flow environment near the liquid injector, and thus to accurately predict the heat load to the injector faceplate. However, to date it is still not feasible to conduct CFD simulations of the detailed flowfield with very complicated geometries such as fluid flow and heat transfer in an injector assembly and through a porous plate, which requires gigantic computer memories and power to resolve the detailed geometry. The rigimesh (a sintered metal material), utilized to reduce the heat load to the faceplate, is one of the design concepts for the injector faceplate of the GEN-II RLV. In addition, the injector assembly is designed to distribute propellants into the combustion chamber of the liquid rocket engine. A porosity model thus becomes a necessity for the CFD code in order to efficiently simulate the flow and heat transfer in these porous media, and maintain good accuracy in describing the flow fields. Currently, the FDNS (Finite Difference Navier-Stokes) code is one of the CFD codes which are most widely used by research engineers at NASA Marshall Space Flight Center (MSFC) to simulate various flow problems related to rocket engines. The objective of this research work during the 10-week summer faculty fellowship program was to 1) debug the framework of the porosity model in the current FDNS code, and 2) validate the porosity model by simulating flows through various porous media such as tube banks and porous plate.

## **Numerical Methodology**

The framework of the FDNS code is an elliptic, finite difference Navier-Stokes flow solver<sup>1-3</sup>, which employs a predictor plus multi-corrector pressure-based solution algorithm. Higher order upwind, total variation diminishing (TVD), or central difference schemes plus adaptive second-order and fourth-order dissipation terms are used to approximate the convection terms of the transport equations. Various matrix solvers, such as vectorized point implicit, conjugate gradient, and generalized minimal residual<sup>4</sup> (GMRES), are provided in the code such that users can select one for a given transport equation. Finite-rate and equilibrium chemistries were incorporated in the code to account for the effect of combustion. Since the FDNS flow solver is a structured code, multi-block, multi-zone options are included in the code so that problems with complex geometries can be analyzed efficiently. The governing equations in curvilinear coordinates solved in the code can be expressed in general form as

$$\frac{1}{J} \frac{\partial \rho q}{\partial t} = - \frac{\partial F_i}{\partial \xi_i} + S_q$$

where  $q$  stands for dependent variables ( $1, u, v, w, h, k, \varepsilon$ , and  $\alpha_n$  which denote unity, velocities in the Cartesian x-, y-, z-direction, enthalpy, turbulence kinetic energy and dissipation rate, and species mass fractions respectively).  $\xi_i, t$ , and  $\rho$  are the curvilinear coordinates, time and fluid density. The numerical flux in the i-direction,  $F_i$ , consists of convective flux,  $Fc_i$ , and a viscous flux,  $Fv_i$ , i.e.

$$F_i = Fc_i + Fv_i \quad , \quad Fc_i = \rho U_i q \quad , \quad Fv_i = -\mu_e G_{ij} \frac{\partial q}{\partial \xi_i}$$

where  $U_i, G_{ij}$ , and  $J$  represent the transformed velocities, diffusion metrics, and Jacobian of the coordinate transformation, respectively. The source terms,  $S_q$ , of the continuity, x-, y-, z-momentums, energy, turbulent kinetic energy and dissipation rate, and species equations

### **Porosity Model**

The porosity model is employed to account for the effects of area/volume blockage and drag force as well as heat source/sink due to the presence of the porous media without resolving the detailed geometry of tiny pores and solid objects. The implementation of the porosity into the CFD code is illustrated as follows. First, the volume porosity ( $\gamma_v$  defined as the ratio of the volume occupied by the fluid to the total volume), and the surface porosity ( $\gamma_i$  defined as the ratio of the surface area in the i-direction available for the flow passage to the corresponding total surface area in the same direction) are introduced into the governing equation and can be expressed as

$$\frac{\gamma_v}{J} \frac{\partial \rho q}{\partial t} = -\frac{\partial \gamma_i F_i}{\partial \xi_i} + \gamma_v S_q$$

Second, a distributed drag force,  $D$ , and a heat flux source/sink term,  $H$ , are added to the right hand side of the momentum equation and the energy equation, respectively, to account for the effect of resistance and heat transfer due to the presence of the porous media. These drag force and heat flux terms were modeled based on geometric parameters and the averaged velocity through the porous media. The drag force  $D$  is defined as

$$D = \frac{1}{2} \rho V_i^2 C_D A$$

where  $C_D$  is the local drag coefficient is a function of types of porous media, local flow speed and geometric parameter. For the flow through an inline or staggered tube bank, empirical correlations<sup>5</sup> in Tables 1 and 2, are incorporated into the code to compute the drag coefficient.

Range	$C_D$
$10^2 < Re_d < 4 \times 10^3$	$0.535 \exp(5.378 Re_d^{-0.345})$
$4 \times 10^3 < Re_d < 6 \times 10^4$	$0.735 - 0.411 \times 10^{-6} Re_d$
$6 \times 10^4 < Re_d < 1 \times 10^6$	$0.621 + 0.169 \times 10^{-5} Re_d - 11.343 \times 10^{-12} Re_d^2 + 16.656 \times 10^{-18} Re_d^3 - 7.377 \times 10^{-24} Re_d^4$
$1 \times 10^6 < Re_d$	0.2735

Range	$C_D$
$10^2 < Re_d < 4 \times 10^3$	$0.417 \exp(4.932 Re_d^{-0.296})$
$4 \times 10^3 < Re_d < 6 \times 10^4$	$0.647 - 0.5 \times 10^{-6} Re_d$
$6 \times 10^4 < Re_d < 1 \times 10^6$	$0.618 + 0.491 \times 10^{-6} Re_d - 6.303 \times 10^{-12} Re_d^2 + 10.694 \times 10^{-18} Re_d^3 - 5.2 \times 10^{-24} Re_d^4$
$1 \times 10^6 < Re_d$	0.2735

Both the drag coefficient model for a perforated plate and the heat flux model are incorporated into the code. These models are detailed in the final report to NASA MSFC TD-64. Due to the space limitation of this report, these models will not be described here. Readers can refer to the final report to TD-64 for the detailed.

## Numerical Results

### Tube Banks

Three flow conditions ( $Re_d = 1000, 5000, \text{ and } 10000$ ) were simulated for the flow through both in-line and staggered tube banks with three different tube spacing ( $a = S_1/d = 2, 1.5, \text{ and } 1.25$ ), where the tube has a diameter of 1 cm. Due to the space limitation of this report, only the result of the staggered tube bank flow is included here. The complete comparison and discussion are detailed in the final report to TD-64. The computational domain and definitions of key parameters are sketched as shown in Figure 1. The comparisons of the Euler number ( $Eu = 2\Delta p / \rho u^2$ ) between the numerical results and the empirical data are plotted as shown in Figure 2. Though the pressure loss is shown to be dependent on the flow blockage; it does not demonstrate the similar trend for various Reynolds number. Later, it was found out the empirical correlation of drag coefficients has less dependence on the Reynolds number than the pressure drop data. Hence the empirical correlation of drag coefficients needs to be fine-tuned in the future to obtain the Reynolds number dependence.

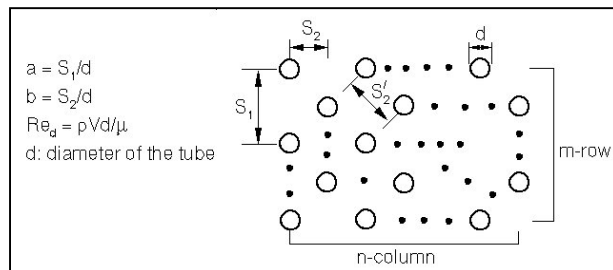


Figure 1: Definition of geometric parameters of the staggered tube bank

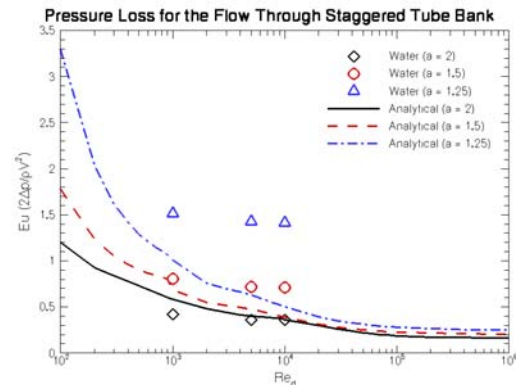


Figure 2: Pressure loss coefficient for the flow through staggered tube banks

### Porous Plates

Numerical simulations were conducted for the flow through a 1"-thickness porous plate (pore diameter = 10  $\mu\text{m}$ , volume porosity = 0.1) with various specific mass fluxes. The numerical result indicates the pressure loss predicted by the porosity model demonstrates a trend similar to the test data for various specific mass fluxes. Due to the proprietary of the test case as well as the space limitation of this report, the data comparison will not be presented here. If interested, readers can refer to the final report to NASA MSFC TD-64.

### Conclusion

The framework of the porosity model in the FDNS-500 code has been verified. The numerical analyses of the tube bank flow demonstrate the qualitative trend of the pressure loss across the tube bank. However, more validations are needed to fine-tune the model to predict both qualitative and quantitative trends for various area porosities and Reynolds numbers. More validations are also needed for the porosity model of the perforated plate to examine the effect of different pore sizes and volume porosities. Due to the limitation of the time, only the empirical correlation for the drag force of the porosity model was verified. The empirical heat transfer correlation of the porosity model needs to be verified in the future.

### Acknowledgements

The author would like to thank my colleagues of Applied Fluid Dynamics Analysis Group (TD64), Transportation Directorate, NASA Marshall Space Flight Center, for their support and valuable information, especially for Kevin Tucker, Jeff West, Marvin Rocker, Jeff Lin, and Roberto Garcia.

### References

1. Chen, Y.S., Liu, J., "FDNS CFD Code Version 500-- Input Data Guide", Engineering Sciences, Inc., Aug. 2000.
2. Chen, Y.S., "Compressible and Incompressible Flow Computations with a Pressure Based Method," AIAA Paper 89-0286, 1989.
3. Cheng, G.C., Chen, Y.S., and Wang, T.S., "Flow Distribution Within the SSME Main Injector Assembly Using Porosity Formulation," AIAA Paper 95-0350, AIAA 33rd Aerospace Sciences Meeting and Exhibit, Jan. 9-12, 1995.
4. Saad, Y., and Schultz, M.H., SIAM Journal of Sci. Stat. Comput., Vol. 7, pp. 856-869, 1986.
5. Zukauskas, A., and Ulinskas, R., "Heat Transfer in Tube Banks in Crossflow," Hemisphere Publishing Co., New York, 1988.